

Revisiting Reactor Anti-Neutrino 5 MeV Bump with ^{13}C Neutral-Current Interaction

Pouya Bakhti,^{1,*} Min-Gwa Park,^{1,†} Meshkat Rajaei,^{1,‡} Chang Sub Shin,^{2,3,4,§} and Seodong Shin^{1,3,¶}

¹*Laboratory for Symmetry and Structure of the Universe, Department of Physics,
Jeonbuk National University, Jeonju, Jeonbuk 54896, Korea*

²*Department of Physics and Institute of Quantum Systems,
Chungnam National University, Daejeon 34134, Korea*

³*Center for Theoretical Physics of the Universe,
Institute for Basic Science, Daejeon 34126, Korea*

⁴*Korea Institute for Advanced Study, Seoul 02455, Korea*

For the first time, we systematically investigate the potential of neutrino-nucleus neutral current interactions with ^{13}C to identify the origin of the 5 MeV bump observed in reactor anti-neutrino spectra in the inverse beta decay process. The distinctive signal is obtained from the de-excitation of $^{13}\text{C}^*$ into the ground state emitting a 3.685 MeV photon in various liquid scintillator detectors. Such an interaction predominantly occurs for the reactor anti-neutrinos within the energy range coinciding with the 5 MeV bump. For a detector that has a capability of 95% level photon and electron separation and small thorium contamination below 5×10^{-17} gr/gr located in a site with an overburden of about a few hundred m.w.e, such as the location of near detectors of RENO and Daya Bay will have a great sensitivity to resolve the 5 MeV bump. In addition, we propose a novel approach to track the time evolution of reactor isotopes by analyzing our ^{13}C signal shedding light on the contributions from ^{235}U or ^{239}Pu to the observed bump. This provides an extra powerful tool in both discriminating the flux models and testing any new physics possibilities for the 5 MeV bump at 3σ to 5σ level with much less systematic uncertainties and assuming 10 kt.year of data collection. Our detector requirements are realistic, aligning well with recent studies conducted for existing or forthcoming experiments.

Introduction. Since its first discovery¹, reactor neutrinos have advanced our comprehension of the lepton sector. Notably, the KamLAND experiment confirmed the neutrino oscillation as the explanation for the solar neutrino problem². Daya Bay³, RENO⁴, and Double Chooz⁵ experiments measured a non-zero value of oscillation parameter θ_{13} . This discovery has opened the possibility of CP violation in neutrino oscillation. Future reactor neutrino experiment JUNO⁶ aims to determine the neutrino mass ordering and achieve sub-percent precision in measuring solar neutrino oscillation parameters, which can be complemented by the liquid scintillator counter at Korean new underground lab, Yemilab^{7,8}, promising precise investigations into solar characteristics.

Probes of neutrino oscillation using reactor neutrinos necessitate accurate theoretical predictions of the neutrino flux. However, its calculation is very complicated and traces its origins to the early days subsequent to the first detection of neutrinos in the Cowan and Reines reactor experiment¹. The Vogel model⁹, employed as the standard flux model for two decades starting from the 1990s, relies on the conversion method and predicts reactor flux measurements based on the Institut Laue-Langevin (ILL) electron spectrum measurements^{10,11}.

Interestingly, the actual neutrino fluxes measured in several short-baseline reactor neutrino experiments with varying fission fractions were smaller than the expected values, which has drawn more careful calculations, such as those by Mueller et al.¹² and Huber¹³. Nonetheless, the predicted fluxes still surpass the observations by about 6% corresponding to a 3σ level discrepancy in the overall energy spectra, now dubbed as the reactor

antineutrino anomaly (RAA)¹⁴.

Moving the focus to a narrower prompt energy range of 4 to 6 MeV, the situation becomes more arduous. In contrast to the deficit in the overall flux, the observed data first reported by RENO¹⁵, and then confirmed by other experiments such as Daya Bay¹⁶, Double Chooz⁵, NEOS¹⁷, Neutrino-4¹⁸, and DANSS (preliminary)¹⁹ at more than 4σ . Moreover, STEREO²⁰ and PROSPECT²¹, utilizing research reactors powered by 100% ^{235}U fuel, have excluded the no 5 MeV bump scenario with more than 3.5σ and 2σ C.L. respectively. This anomaly is called the *5 MeV bump*²².

Reactor electron anti-neutrinos are predominantly detected through the inverse beta decay (IBD) reaction, offering distinct advantages such as a large cross-section and a clear coincidence of the prompt positron annihilation and the delayed neutron capture γ -ray emission. The detection threshold for IBD is 1.8 MeV. The previously mentioned 5 MeV bump is observed from IBD, which means the positron energies peak around 5 MeV beyond the expectation by Huber-Mueller (HM). To further investigate its origin, whether it is coming from a miscalculation of the flux, new physics, or IBD systematic, employing another detection approach is advantageous. In this letter, for the first time, we propose to use the neutral current (NC) interaction of neutrinos with ^{13}C isotope ubiquitous with mostly about 1.1 % abundance in the carbon-based liquid scintillator (LS) detectors to identify the 5 MeV bump alternatively to the IBD. The interaction threshold is 3.685 MeV, resulting in the excitation of ^{13}C nuclei to their first excited state. Then, a 3.685 MeV γ -ray emits from prompt de-excitation of $^{13}\text{C}^*$

nuclei, creating a distinctive signal. Note that NC interactions are flavor blind and are not affected by neutrino oscillation parameter uncertainties. However, other types of interactions such as neutrino-electron elastic scattering (ES) and coherent elastic neutrino-nucleus scattering (CE ν NS), which benefit from low energy thresholds, suffer from large systematic uncertainty, and detecting signals above the background poses significant challenges rendering them less suitable for studying the 5 MeV bump. It is worth noting that CC and NC interactions of deuterons can be alternative methods in experiments with a sufficient quantity of heavy water²³.

Expected event spectrum. The cross-section for the NC interaction of neutrinos with ^{13}C is given by²⁴:

$$\sigma(E_\nu) = [a_1(E_\nu - Q) + a_2(E_\nu - Q)^2] \times 10^{-44} \text{cm}^2 \quad (1)$$

where $Q = 3.685$ MeV is the energy threshold, $a_1 = 0.122$, and $a_2 = 1.26$ are constants^{25,26}. Figure 1 shows the cross-section represented by the dashed green curve. Notice that for light nuclei such as ^{13}C , there is a good agreement between theory and experiment. Hence, we expect the cross-section uncertainty would follow the best theoretical calculations to the 1% level^{27,28} although its experimental measurement lacks so far. Various experiments, including reactor neutrino interactions, solar neutrino observations at JUNO²⁸ and Yemilab^{7,8}, and electron anti-neutrino production at IsoDAR^{7,29} can measure the cross-section in the near future³⁰.

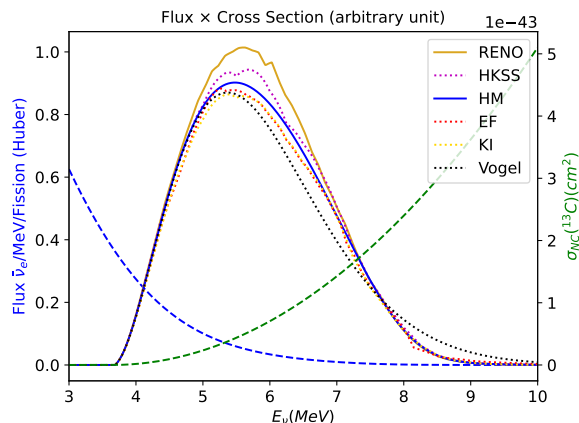


FIG. 1. The flux of reactor neutrinos based on the Huber-Mueller (HM) model is depicted by a dashed blue curve^{12,13}. The cross-section of NC $\bar{\nu}_e - ^{13}\text{C}$ is shown by a dashed green curve²⁴. Additionally, the product of the reactor neutrino flux and the cross-section is evaluated across several reactor models, including HKSS³¹, HM, EF³², KI³³, and Vogel⁹, and for the reconstructed flux from RENO³⁴. These calculations assume identical fission fractions as reported for near detector of RENO³⁴.

In Fig. 1, we present the flux of reactor neutrinos with the dashed blue curve, assuming the HM model^{12,13} and considering the average fission fractions at near detector of RENO³⁴ as follows: 0.571 for ^{235}U , 0.073 for ^{238}U ,

Experiments	P(GW)	m(t)	Baseline(m)	events/yr
Daya Bay (near/far)	17.4/17.4	80/80	578.7/1638	88/11
RENO (near/far)	16.4/16.4	16/16	420/1400	38/3.4
PROSPECT-II	3	4.8	25	491
JUNO-TAO	4.6	2.8	30	305
NEOS	2.8	1	24	103

TABLE I. A summary of power, mass, baseline and the expected number reactor $\bar{\nu} ^{13}\text{C}$ NC events for various experiments.

0.3 for ^{239}Pu , and 0.056 for ^{241}Pu . Other reactor models are not illustrated as they overlap with each other. Moreover, we show the product of the flux and the $\bar{\nu}_e$ interaction cross-section with ^{13}C , considering various flux models such as HM, Vogel⁹, KI (Kurchatov Institute)³³, EF (Estienne-Fallot)³², and HKSS (Hayen-Kostensalo-Severijns-Suhonen)³¹, as well as the reconstructed number of events considering excess events at RENO¹⁵. For a review of different models, see^{35,36}.

As demonstrated in Fig. 1, a significant number of events falls within the neutrino energy range of 4.5 to 7.5 MeV, coinciding with the 5 MeV bump anomaly. This interaction thus presents a novel opportunity to investigate the differentiate among reactor flux models, offering a new channel testing the phenomenon. The ratios of events for the Vogel, KI, EF, and HKSS models to HM model are 0.96, 0.96, 0.97, and 1.03, respectively³⁷. Assuming all the excess events in the IBD measurements as reported in Ref.³⁶ are caused by a higher flux, the experimental events involving ^{13}C will likely be 4% to 8% higher than predicted by the HM model. In the case of RENO³⁴, as demonstrated in Fig. 1, it is 8% higher than the HM model events. Hence investigations identifying the origin of the 5 MeV bump rely on how much we can reduce the uncertainties in the current/future experiments.

We present the annual number of ^{13}C events for the reference current or near-future reactor neutrino experiments in Table I. The number of events is directly proportional to reactor power and detector mass, and the inverse of the square of the baseline. Assuming the average fission fraction reported by near detector of RENO³⁴ and employing the HM model, the annual number of ^{13}C events in a commercial reactor is estimated to be approximately $22 \times (\text{Power/GW}) \times (\text{Mass/kt}) / (\text{Baseline/km})^2$.

Background analysis. The main backgrounds for the 3.685 MeV photon signal are the misidentification of electrons from ES or IBD events by the reactor neutrinos which scale together with the signal events, thallium (^{208}Tl) β decays due to the thorium (^{232}Th) contamination in LS, the environmental backgrounds from cosmic muon spallation or external radioactivity, and the solar neutrinos if $(\text{Baseline/km})^2 \gg (\text{Power/GW})$.

Assuming $5\%/\sqrt{E}$ (MeV) energy resolution, we define our region-of-interest (ROI) as $3.685 \text{ MeV} \pm \text{FWHM}$ (0.1 MeV). Notice that for JUNO-TAO the energy resolution is $1\%/\sqrt{E}$ (MeV)³⁸. Adopting the neutron veto capabil-

ity along with a fiducial volume cut in Ref.³⁹, we expect the misidentified IBD events in our ROI would be 0.1% of the total events, resulting in the sum of misidentified ES and IBD events is about 6 times the signal events. For the current level reactor neutrino experiments, discrimination of photon and electron (γ/β) in our ROI is almost impossible except for JUNO and JUNO-TAO which can have 90% level γ/β discrimination efficiency in the energy range of 1.25 - 1.75 MeV⁴⁰. Also, a future detector design LiquidO is expected to achieve even better efficiency⁴¹. Conventionally the γ/β discrimination efficiency increases with energy thus for JUNO-TAO and future experiments we have assumed 95% γ/β discrimination. For JUNO-TAO with a good energy resolution and γ/β discrimination, the number of ES and IBD misidentified background is expected to be twenty times smaller than signal³⁸.

Another source of backgrounds below 5 MeV is beta decays of ^{208}Tl from the ^{232}Th chain with simultaneous emissions of α and β . We expect around one ^{208}Tl event in ROI at 1kt LS every day for a LS detector with ^{232}Th contamination at the level of 5×10^{-17} gr/gr which is KamLAND level purity. Nevertheless, utilizing coincidence of α decay in the ^{232}Th chain and β decay of ^{208}Tl , so-called ^{232}Th series tagging 80% and 99% of this background can be rejected with KamLAND and JUNO respectively^{42,43}. Even conservatively, assuming 80% rejection of the ^{232}Th background is not the dominant one.

Environmental backgrounds such as cosmic muon spallation and external radioactivities from detector walls and surrounding rocks also exist. However, an overburden of a few hundred m.w.e. along with muon veto and fiducial volume cut can reduce those backgrounds to the 5% and negligible level, respectively³⁹. After muon veto cuts, we expect around 5 muon spallation events in the ROI at 1 kt LS every day. These environmental backgrounds can be further mitigated using reactor on-off time and the γ/β discrimination. Note that there can be extra background events by the high energy photons and fast neutrons from the reactor for very short baseline experiments such as NEOS, JUNO-TAO, and PROSPECT II. Exactly estimation of this background is out of the scope of this paper.

To prove the feasibility of our proposal searching for the reactor antineutrino NC scattering with ^{13}C , we assume future reference detectors where our background rejection scheme with the γ/β separation efficiency 95% (for the ES, IBD, and environmental backgrounds) is applied are installed in the location of the near halls of RENO, Daya Bay, and the far hall of the proposed SuperChooz. For simplicity, we temporarily name those RENO+ (1kt LS), Daya Bay+ (1kt LS), and Chooz+ (10kt LS), respectively. Note that our background rejection scheme, which is based on ongoing studies, is not too ambitious; e.g., the ^{208}Tl background rejection rate is conservatively assumed and we do not apply the reactor on-off time cut. Their overburden are 120 m.w.e., 265 m.w.e., and 300 m.w.e., in the given order. For

Experiments	events	ES+IBD	Muon spallation	^{208}Tl
RENO+	2095	610	900	72
Daya Bay+	1530	460	180	72
Chooz+	1850	550	900	720

TABLE II. Number of reactor antineutrino ^{13}C events and backgrounds every active year in our ROI. See the main texts for the details of each reference detector.

the muon flux of RENO and Daya Bay near hall, we assumed 10 and 2 times larger muon spallation background scaled from Ref.³⁹, respectively. The expected signal (with 100% signal acceptance) and background numbers every active year in our ROI are listed in Table II. The ratio $N_{\text{background}}/N_{\text{signal}}$ is 76%, 47%, and 117% for each detector in the given order, showing that our signal can be probed with enough sensitivities.

Flux measurement sensitivities. Equipped with the background analysis schemes, now we explore the flux measurement sensitivities of various experiments including our proposed detectors from the $\bar{\nu} - ^{13}\text{C}$ NC interactions. For simplicity, we adopt the three background scenarios: $N_{\text{background}}/N_{\text{signal}} = 6, 1, \text{ and } 0$. The first scenario is obtained by assuming all the backgrounds are from IBD and ES of the reactor neutrinos with the zero γ/β separation efficiency as discussed previously while ignoring others, which is still conservative. The second scenario is well justified from Table II. The third scenario is chosen to show the best-case scenario. The dotted, dashed, and solid curves in Fig. 2 correspond to the 1σ C.L. sensitivities for the first, second, and third background scenarios, respectively. The red, blue, and green curves are drawn additionally considering the systematic uncertainties of 0%, 1%, and 3%, in the given order. Note that the separation of those red, blue and green curves becomes more larger for the scenarios with smaller backgrounds. The vertical dotted lines correspond to the statistics of various past, current, and future experiments along with our new proposed detectors. For the past experiments (RENO and Daya Bay) we accounted for data collected over the entire duration of the experiment. However, for current and future experiments, we have considered 10 years of data collection. The light grey shaded region is the level of flux measurement uncertainties (4-8%) which can start to separate different theoretical flux models at 1σ . As can be seen in Fig. 2, the flux measurement sensitivity of RENO which could not separate photon and electron events, corresponding to our first background scenario at least (dot-dashed curves), was worse than 14%. This is definitely beyond the light grey shaded region, which means that RENO did not have sensitivity to distinguish different flux models from the $\bar{\nu}_e - ^{13}\text{C}$ NC interactions. On the other hand, our proposed reference detector at the near hall site of RENO, called RENO+, is expected to reach about 4% sensitivity clearly distinguishing the flux models, after about 3000 events that corresponds to 1.5 years of active running

even with the 3% level systematic uncertainty.

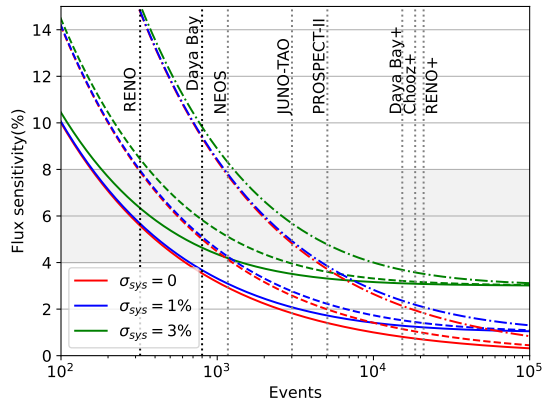


FIG. 2. Signal acceptance is universally assumed to be 100% for simplicity. The dot-dashed, dashed, and solid curves stand for our first, second, and third background scenarios, i.e., $N_{\text{bkg.}}/N_{\text{sig.}} = 6, 1, 0$, respectively. For red, blue and green curves, we have considered zero, 1% and 3% systematic uncertainty respectively. The number of events of RENO and Daya Bay are from their final data while the others are from assuming ten years of data taking. The light grey shaded region (4-8%) is the level of flux measurement uncertainties that can start to separate different theoretical flux models at 1σ .

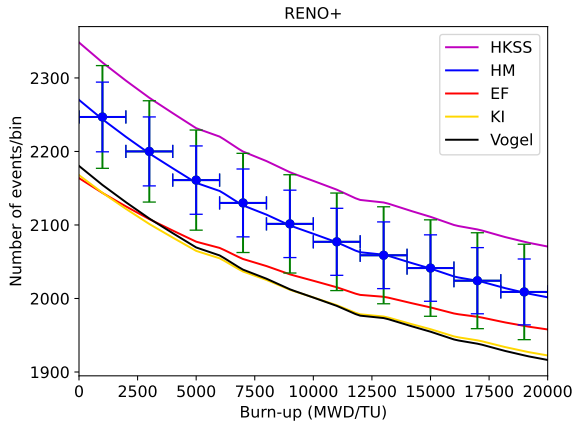


FIG. 3. Number of events versus burn up in the unit of megawatt-day over thermal unit (MWD/TU) at RENO+ assuming 10 years of data taking.

Fission fraction evolution. Now we discuss another powerful analysis method identifying the origin of the 5 MeV bump, the fission fraction evolution, which is less affected by the systematic uncertainties. As can be observed from Fig. 3, assuming fission fractions evolution in Daya Bay⁴⁴, we can distinguish various flux models by observing the time evolution of the reactor. The blue and green error bars correspond to 1σ statistical only and statistical plus 1% systematic uncertainties

respectively, assuming ten years of data taking. Without considering systematics and background, RENO+ is expected to achieve a 5σ sensitivity in discriminating between the HKSS and HM models. Considering 1% and 3% systematic uncertainties and including background, RENO+ can distinguish between HKSS and KI at 6σ and 4.5σ respectively, while it discriminate between HKSS and HM at 2σ to 2.5σ . Daya Bay+ and Chooz+ have a similar sensitivities. The near future experiments JUNO-TAO and PROSPECT-II have 3σ and 4σ sensitivities, respectively, to distinguish between HKSS and KI models assuming 1% systematics and neglecting the background. Moreover, under the assumption of a fixed flux model, there is a 14% difference in the number of ^{13}C events between the start and end of the fuel cycle for all the demonstrated models except EF model which is 10%. This reduced rate of evolution is a sufficient discrimination between EF model and the other models. Let us emphasize that the only relevant systematic in this approach is the fission fraction systematic. Another crucial question is how much different isotopes contribute to this bump²². Since the ^{239}Pu fission fraction increases in time, by observing ^{13}C events during fuel evolution, one can find the contribution of different isotopes to the 5 MeV bump. A steeper decrease in the number of events indicates a larger theoretical deviation from the experimental data regarding ^{239}Pu . Conversely, a shallower slope suggests a greater influence of ^{235}U in the observed bump. A combination of IBD and ^{13}C will make it more accessible to investigate the contribution of the different isotopes to the 5 MeV bump. This indicates the potential to observe fuel evolution within a reactor, as well as to measure fission fractions during the fuel cycle or the beta spectrum ratio between ^{235}U and ^{239}Pu . Notice that the fission fraction of ^{238}U remains nearly constant, while that of ^{241}Pu exhibits a roughly linear relationship with the ^{239}Pu fraction.

Measuring the evolution of reactor fuel is crucial for distinguishing between the new physics hypothesis and various flux models as explanations for the RAA or the 5 MeV bump. If it is caused by new physics effects such as sterile neutrino oscillations, then the observed deficit (RAA) or excess (5 MeV bump) should remain consistent across all fission isotopes. On the other hand, if the anomalies stem from errors in reactor modeling, one might observe variations in the deficit among different fission isotopes and the observed data would be consistent with the HKSS expectation, the magenta curve in Fig. 3. This can be achieved by comparing the event ratios observed at detectors with different baselines, or through a combination of experiments with varying baselines while considering an average neutrino energy of 6 MeV. Combining our analysis methods, both from Fig. 2 and 3, we expect that the new physics hypothesis can be tested with 2.5σ to 5σ level significance even with the background level $N_{\text{background}} = N_{\text{signal}}$ and 1% systematic uncertainty.

Concluding remarks. We have revisited the origin of the 5 MeV bump for the first time using ^{13}C in liquid scintillators, which has a distinctive monochromatic 3.685 MeV photon as the signal with proper background reduction strategies and enough statistics of data taking. With a few hundred m.w.e such as the locations of near detectors of RENO and Daya Bay, and employing a 10 kt-year data collection, we anticipate achieving a sensitivity ranging from 2σ to 5σ for identifying the origin of the 5 MeV bump, whether it is from the reactor neutrino flux or exotic phenomena from a new physics theory, which is extremely powerful and generically applied. This expectation holds under the assumption of 1 to 3 percent systematics, with a comparable signal to background ratio which can be achievable with a high level of photon and electron discrimination efficiency. Furthermore, these experiments hold significant potential to discern the contribution of various isotopes to the bump, taking into

account the time evolution of the reactor and sensitivity to fuel evolution. Effectively controlling and minimizing environmental background in very short baseline experiments such as JUNO-TAO, PROSPECT-II and NEOS could greatly enhance the sensitivity of these experiments in resolving 5 MeV bump, although further dedicated study is needed. From our analysis proposals, we expect to shed light on resolving the problems of the reactor neutrino fluxes.

Acknowledgements. This work is supported by the Basic Research Laboratory Program of the National Research Foundation (NRF) of Korea with Grant No. NRF-2022R1A4A5030362. The work of PB, MGP, MR, and SS are additionally supported by the NRF with Grant No. NRF-2020R1I1A3072747. CSS is also supported by the NRF with Grant No. NRF-2022R1C1C1011840. CSS and SS are partly supported by IBS-R018-D1.

* pouya_bakhti@jbnu.ac.kr

† mgpark@jbnu.ac.kr

‡ meshkat@jbnu.ac.kr

§ csshin@cnu.ac.kr

¶ sshin@jbnu.ac.kr

¹ C. L. Cowan, F. Reines, F. B. Harrison, H. W. Kruse, and A. D. McGuire, *Science* **124**, 103 (1956).

² A. Gando *et al.* (KamLAND), *Phys. Rev. D* **88**, 033001 (2013), arXiv:1303.4667 [hep-ex].

³ D. Adey *et al.* (Daya Bay), *Phys. Rev. Lett.* **121**, 241805 (2018), arXiv:1809.02261 [hep-ex].

⁴ G. Bak *et al.* (RENO), *Phys. Rev. Lett.* **121**, 201801 (2018), arXiv:1806.00248 [hep-ex].

⁵ Y. Abe *et al.* (Double Chooz), *JHEP* **10**, 086 (2014), [Erratum: *JHEP* **02**, 074 (2015)], arXiv:1406.7763 [hep-ex].

⁶ F. An *et al.* (JUNO), *J. Phys. G* **43**, 030401 (2016), arXiv:1507.05613 [physics.ins-det].

⁷ S.-H. Seo *et al.*, (2023), arXiv:2309.13435 [hep-ex].

⁸ P. Bakhti, M. Rajaei, S.-H. Seo, and S. Shin, (2023), arXiv:2307.11582 [hep-ph].

⁹ P. Vogel and J. Engel, *Phys. Rev. D* **39**, 3378 (1989).

¹⁰ K. Schreckenbach, H. R. Faust, F. von Feilitzsch, A. A. Hahn, K. Hawerkamp, and J. L. Vuilleumier, *Phys. Lett. B* **99**, 251 (1981).

¹¹ F. Von Feilitzsch, A. A. Hahn, and K. Schreckenbach, *Phys. Lett. B* **118**, 162 (1982).

¹² T. A. Mueller *et al.*, *Phys. Rev. C* **83**, 054615 (2011), arXiv:1101.2663 [hep-ex].

¹³ P. Huber, *Phys. Rev. C* **84**, 024617 (2011), [Erratum: *Phys. Rev. C* **85**, 029901 (2012)], arXiv:1106.0687 [hep-ph].

¹⁴ G. Mention, M. Fechner, T. Lasserre, T. A. Mueller, D. Lhuillier, M. Cribier, and A. Letourneau, *Phys. Rev. D* **83**, 073006 (2011), arXiv:1101.2755 [hep-ex].

¹⁵ J. H. Choi *et al.* (RENO), *Phys. Rev. Lett.* **116**, 211801 (2016), arXiv:1511.05849 [hep-ex].

¹⁶ F. P. An *et al.* (Daya Bay), *Phys. Rev. Lett.* **116**, 061801 (2016), [Erratum: *Phys. Rev. Lett.* **118**, 099902 (2017)], arXiv:1508.04233 [hep-ex].

¹⁷ Y. J. Ko *et al.* (NEOS), *Phys. Rev. Lett.* **118**, 121802 (2017), arXiv:1610.05134 [hep-ex].

¹⁸ A. P. Serebrov *et al.*, *Phys. Rev. D* **104**, 032003 (2021), arXiv:2005.05301 [hep-ex].

¹⁹ M. Danilov, PoS **ICHEP2022**, 616 (2022), arXiv:2211.01208 [hep-ex].

²⁰ H. Almazán *et al.* (STEREO), *J. Phys. G* **48**, 075107 (2021), arXiv:2010.01876 [hep-ex].

²¹ M. Andriamirado *et al.* (PROSPECT, (PROSPECT Collaboration)*), *Phys. Rev. Lett.* **131**, 021802 (2023), arXiv:2212.10669 [nucl-ex].

²² P. Huber, *Phys. Rev. Lett.* **118**, 042502 (2017), arXiv:1609.03910 [hep-ph].

²³ A review of detection channels for reactor antineutrinos is found in Ref.⁴⁵.

²⁴ T. Suzuki, A. B. Balantekin, and T. Kajino, *Phys. Rev. C* **86**, 015502 (2012), arXiv:1204.4231 [nucl-th].

²⁵ M. Fukugita, Y. Kohyama, and K. Kubodera, *Phys. Lett. B* **212**, 139 (1988).

²⁶ T. Suzuki, A. B. Balantekin, T. Kajino, and S. Chiba, *J. Phys. G* **46**, 075103 (2019), arXiv:1904.11291 [nucl-th].

²⁷ B. R. Barrett, P. Navrátil, and J. P. Vary, *Prog. Part. Nucl. Phys.* **69**, 131 (2013).

²⁸ J. Zhao *et al.* (JUNO), (2022), arXiv:2210.08437 [hep-ex].

²⁹ J. Alonso *et al.*, *Phys. Rev. D* **105**, 052009 (2022), arXiv:2111.09480 [hep-ex].

³⁰ P. Bakhti, M.-G. Park, M. Rajaei, C. S. Shin, and S. Shin, .

³¹ L. Hayen, J. Kostensalo, N. Severijns, and J. Suhonen, *Phys. Rev. C* **100**, 054323 (2019), arXiv:1908.08302 [nucl-th].

³² M. Estienne *et al.*, *Phys. Rev. Lett.* **123**, 022502 (2019), arXiv:1904.09358 [nucl-ex].

³³ V. Kopeikin, M. Skorokhvatov, and O. Titov, *Phys. Rev. D* **104**, L071301 (2021), arXiv:2103.01684 [nucl-ex].

³⁴ S. G. Yoon *et al.* (RENO), *Phys. Rev. D* **104**, L111301 (2021), arXiv:2010.14989 [hep-ex].

³⁵ C. Giunti, Y. F. Li, C. A. Ternes, and Z. Xin, *Phys. Lett. B* **829**, 137054 (2022), arXiv:2110.06820 [hep-ph].

³⁶ C. Zhang, X. Qian, and M. Fallot, *Prog. Part. Nucl. Phys.* **136**, 104106 (2024), arXiv:2310.13070 [hep-ph].

- ³⁷ Note that the HKSS model is introduced to fit the 5 MeV bump.
- ³⁸ A. Abusleme *et al.* (JUNO), (2020), arXiv:2005.08745 [physics.ins-det].
- ³⁹ J. M. Conrad, J. M. Link, and M. H. Shaevitz, Phys. Rev. D **71**, 073013 (2005), arXiv:hep-ex/0403048.
- ⁴⁰ H. Rebber, L. Ludhova, B. S. Wonsak, and Y. Xu, JINST **16**, P01016 (2021), arXiv:2007.02687 [physics.ins-det].
- ⁴¹ A. Cabrera *et al.* (LiquidO), Commun. Phys. **4**, 273 (2021), arXiv:1908.02859 [physics.ins-det].
- ⁴² T. Hachiya (KamLAND), J. Phys. Conf. Ser. **1468**, 012257 (2020).
- ⁴³ A. Abusleme *et al.* (JUNO), Chin. Phys. C **45**, 023004 (2021), arXiv:2006.11760 [hep-ex].
- ⁴⁴ F. P. An *et al.* (Daya Bay), Chin. Phys. C **41**, 013002 (2017), arXiv:1607.05378 [hep-ex].
- ⁴⁵ X. Qian and J.-C. Peng, Rept. Prog. Phys. **82**, 036201 (2019), arXiv:1801.05386 [hep-ex].